Raman Vibrational Studies of Syndiotactic Polystyrene. 1. Assignments in a Conformational/Crystallinity Sensitive Spectral Region

Ewen J. C. Kellar,* Costas Galiotis, and Edgar H. Andrews

Department of Materials, Queen Mary and Westfield College, University of London, Mile End Road, London E1 4NS, England

Received June 2, 1995; Revised Manuscript Received December 18, 1995[⊗]

ABSTRACT: A detailed analysis of the Raman spectrum of syndiotactic polystyrene, sPS, in the region 600−850 cm^{-1} has been undertaken. As sPS exhibits considerable polymorphism, spectra of various preparations including melt-crystallized sPS (α/β form), solvent-crystallized sPS (γ/δ forms), and quenched glassy material were studied. The ν_1 vibration of the phenyl ring (ring breathing mode) has been shown to manifest itself through the presence of two peaks resulting from local conformational changes in the alkyl backbone. The peak centred around 773 cm^{-1} has been assigned to an all-trans backbone sequence whereas the higher frequency feature at ∼798 cm^{-1} is attributed to mixed trans/gauche conformations. For comparison the spectrum of atactic polystyrene was also studied, and the presence of a weak shoulder is assigned to a syndiotactic all-trans component within the polymer. Further study of a cross section of molded material exhibiting a skin/core structure reveals the continuous way in which the relative size, position, width, and intensity of these features vary with changing crystallinity.

Introduction

Syndiotactic polystyrene (sPS) can now be synthesized to a very high degree of stereospecificity (>96%)[1]. Unlike its isotactic counterpart (iPS), sPS crystallizes at a relatively high rate to a level of ∼60% and has a melting point of 270 °C. Previous work has shown that it can exist in four main crystalline polymorphic structures, designated α, β, γ, and δ.[2,3] The α and β forms have been shown to have an all-trans planar zigzag $(tttt)_n$ backbone conformation, whereas the γ and δ forms have a helical (trans, trans, gauche, gauche, $(ttg^+g^+)_n$) backbone conformation.[4] The α and β forms are the primary crystalline polymorphs and result from different thermal and pressure treatments above T_g. The α form has been shown to exist in a hexagonal[5,6] or perhaps rhombohedral[7] structure arising from groups of backbone triads, whereas the β form packs in an orthorhombic structure.[8] The γ and δ forms can only be formed from solvent swelling of glassy sPS and have been shown to have effectively the same monoclinic crystal structure.[9] The δ form incorporates solvent molecules trapped within the interstatial spaces of the crystal structure and is stable up to ∼120 °C. Heating the δ form above this temperature drives out the solvent molecules leaving the same crystal structure in which the sites are now vacant. A solid phase transformation of the γ form to the α form is possible at around 180 °C. The complex interconversion between the various physical forms of sPS is demonstrated in Figure 1.

A number of vibrational spectroscopic studies have been carried out on sPS, looking at the different polymorphs and transformations between them.[10−18] Important differences have been observed between the groups of sPS polymorphs, especially with infrared spectra. A very characteristic peak at 1222 cm^{-1} has been observed for samples containing the all-trans conformation and has been assigned to the presence of very long all-trans conformations which do not exist in the helical form.[1,10] Henceforth the 1222 cm^{-1} band and other spectral features have been used to estimate

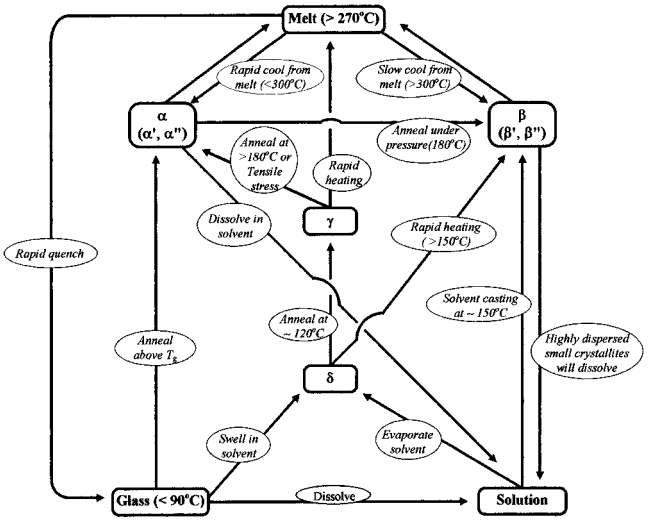

Figure 1. Schematic representation of the complex interconversion between the various physical forms of sPS.

degree of crystallinity,[11] type of crystallinity,[12−14] and rate of crystallization.[15]

Reynolds and Hsu[16] have carried out a normal vibrational analysis of sPS comparing their calculated results with infrared and Raman spectra on drawn fully annealed samples (all-trans form). The calculated frequencies agree well with observed bands, and some features such as the 1222 cm^{-1} band are identified as being unique to the syndiotactic isomer. Large intensity changes are found for some features upon annealing and drawing, with peaks at 943, 934 (infrared), and 800 (Raman) cm^{-1} disappearing totally with such treatments. These peaks are also found to be absent from the calculated results of crystalline sPS (α/β form), thus providing good evidence that these features are not derived from all-trans conformations. A study was carried out by Nyquist et al.[17] comparing the vibrational spectra (Raman and infrared) for sPS (all-trans and helical) with those of iPS, atactic polystyrene (aPS), and toluene. From these comparisons they were able to make partial assignments for both of the sPS polymorphs. Some of their assignments suggested that the

[⊗] Abstract published in *Advance ACS Abstracts,* February 15, 1996.

S0024-9297(95)00772-8 CCC: $12.00

crystal structure of the all-trans polymorph may not be isomorphous with C_{2v} symmetry. The authors appear to make no distinction between the two known polymorphs which have the all-trans conformation. In a paper by Kobayashi et al.,[18] a variety of techniques were used including Raman and infrared spectroscopy to study the differences and transformation between the helical and all-trans forms of sPS. By comparing the crystalline samples, they observed a major difference in the 700−800 cm^{-1} region of the Raman spectrum. For the all-trans material, a strong sharp peak was present at 770 cm^{-1} together with a broad weaker feature at ∼795 cm^{-1}, but in the case of the helical crystal sample the strong broad feature at 798 cm^{-1} now dominated a much weaker peak at 769 cm^{-1}. The sharp 770 cm^{-1} band was attributed to the presence of the all-trans conformation and the 798 cm^{-1} feature to the presence of gauche conformations.

In this work, the first of a series of papers on sPS, an analysis of all the spectral features of sPS in the region 600−800 cm^{-1} is undertaken. The effects of crystal type and degree of crystallinity upon the spectral characteristics such as peak position, intensity, and breadth are examined in detail. It is found that two peaks corresponding to the ν_1 vibrational mode can be clearly identified with one uniquely assigned to an all-trans syndiotactic sequence. Somewhat similar results are derived from aPS thus implying the presence of a syndiotactic component within the atactic polymer. The presence of such a feature allows for the possibility of relating Raman spectral data in this region to the degree of crystallinity, at least for the all-trans form, for sPS.

Experimental Section

Specimen Preparation. Samples of extruded/quenched sPS film were kindly provided by Dow Chemicals Co. Due to the high rate of crystallization observed for sPS, it is not possible to obtain material of zero crystallinity even with quenching; hence the "amorphous" samples provided have a residual crystallinity of ∼11−15% as determined by DSC analysis. Fully crystalline (∼60%) sPS (α/β form) was obtained by annealing a 300 μm amorphous extruded film of sPS at 160 °C for 2 h. Helical (γ/δ) sPS samples were obtained by swelling amorphous sPS film in $CHCl_3$ for 1 h and then drying the sample at 120 °C for 12 h in a vacuum oven to obtain the δ form and heating for a further 5 h at 160 °C in a vacuum oven to derive the γ form. An experimental plaque of compression-molded sPS which was quenched in ice water showing a clear glassy skin and crystalline core was also provided by Dow Chemicals Co. The thickness of the plaque was ∼3 mm. A section of the plaque was cut, and the surface parallel to the long axis of the bar and transverse to the top plane of the bar was carefully polished. Raman spectra were taken at intervals along the polished surface. An ultramicrotome, using a glass knife, enabled thin (∼1 μm) sections to be taken of this surface which were subsequently examined under a Zeiss microscope between crossed polarizers. Atactic polystyrene was obtained from University of North London Polymer Technology Unit. All the sample surfaces were prepared using decreasing grades (increasing fineness) of carborundum paper followed by polishing using a SiO_2 suspension in water.

Laser Raman Spectroscopy. Raman spectra were taken with the 514.5 nm line of an argon ion laser. A modified Nikon microscope was used to focus the incident laser beam to a 2 μm spot on the sample surface. The 180° backscattered light was collected by the microscope objective and focused on the entrance slit of a SPEX 1877 triple monochromator. A Wright Instruments MPP peltier-cooled charge-coupled device (CCD) was employed as a photon-counting system for recording of the Raman spectra. All the Raman frequency values were derived by fitting Lorentzian routines to the CCD raw data.

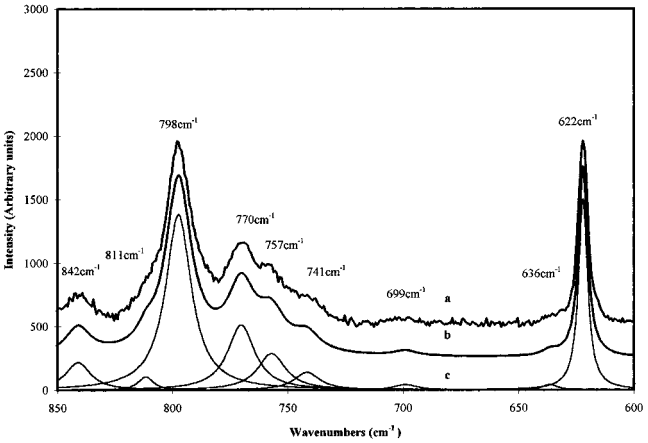

Figure 2. Raman spectra of sPS (glass form): (a) raw data, (b) sum of curves, and (c) fitted curves.

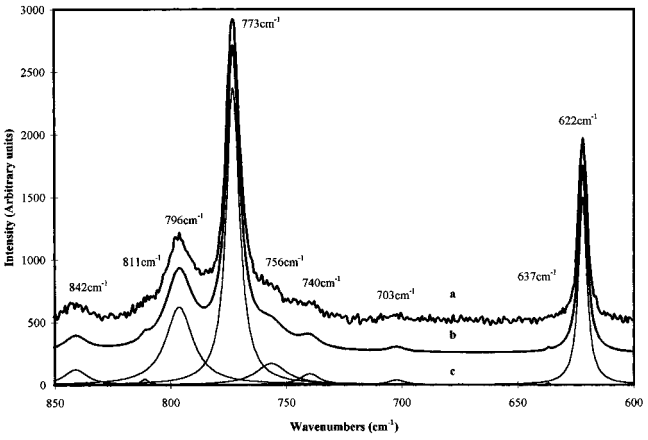

Figure 3. Raman spectra of sPS (all-trans form): (a) raw data, (b) sum of curves, and (c) fitted curves.

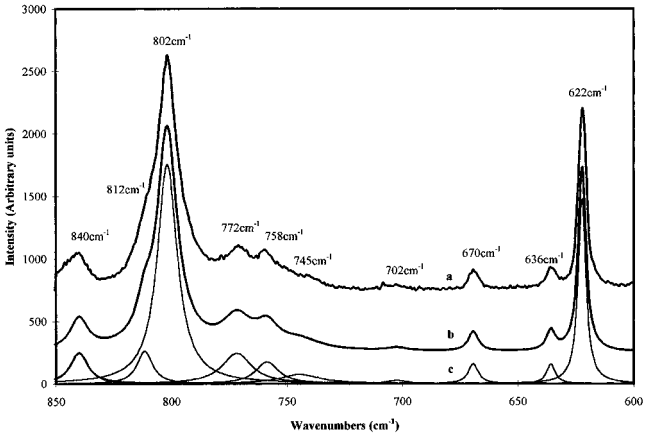

Figure 4. Raman spectra of sPS (helical form): (a) raw data, (b) sum of curves, and (c) fitted curves.

Results and Discussion

The Raman spectra of sPS (glass, all-trans, and helical) and aPS are shown in Figures 2−5 together with the best fit and component peaks. The fitting reveals a remarkable consistency throughout all the samples, in keeping with the syndiotactic nature of the polymer (even for aPS). Careful analysis of published literature in view of the results presented here enabled us to almost completely assign all the spectral features in this region. The assignments are given in Table 1, using both Wilson and Hertzberg nomenclature, but in the discussion only the Wilson format is used. Six fundamental vibrational modes can be identified, ν_1, ν_{6b}, ν_{11},

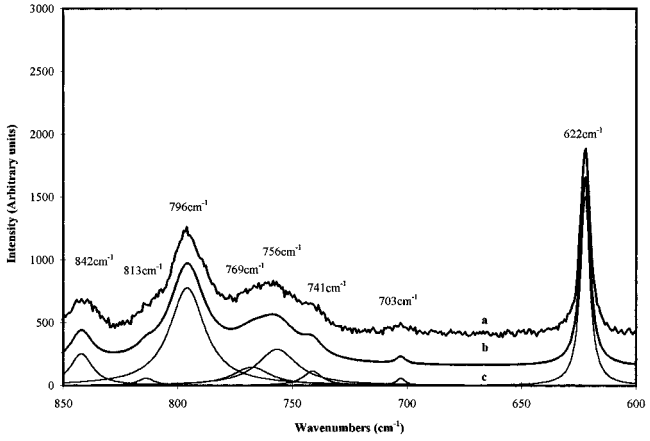

Figure 5. Raman spectra of aPS: (a) raw data, (b) sum of curves, and (c) fitted curves.

ν_{10a}, ν_4, and $\beta_{as}(CH_2)$. The first two are derived from in-plane vibrations of the phenyl ring and the rest from out of plane modes or backbone motions shown in Figure 6.

***ν*$_1$ Vibrational Mode.** Due to the highly symmetric nature of the ν_1 vibration of the phenyl ring (Figure 6), it is not surprising that considerable 'substituent' effects can arise depending upon the nature and conformation of the local polymer backbone. In the case of sPS, two dominant conformations have been shown to exist,[19] namely, $(tttt)_n$ and the slightly higher energy $(ttg^+g^+)_n$ conformation. Amorphous/glassy sPS clearly gives rise to a more mixed set of trans and gauche states. Previous work[18] has shown that sPS can give rise to two distinct ν_1 vibrational peaks, a lower frequency peak deriving from $(tttt)_n$ sequences and a higher frequency one due to a mixture of trans and gauche states.

Jasse et al.[19] looked at the influence of conformational structure on the ν_1 vibration of the phenyl ring in aPS, iPS, and two model compounds of PS using Raman spectroscopy. Their findings are summarized in Table 1. The model compounds were 2,4-diphenylpentane and 2,4,6-triphenylheptane, namely, the PS dimer and trimer, respectively. The trimer was separated into three fractions, isotactic, heterotactic, and syndiotactic, of which the syndiotactic isomer was found to crystallize. Analysis of the spectra showed that the isomers exhibiting total or partial syndiotactic character gave rise to two polarized peaks which could both be assigned to the ν_1 vibration. The crystalline syndiotactic isomer had one main peak at 763 cm^{-1} with a higher frequency shoulder, and the liquid analogue revealed two distinct peaks at 763 and 789 cm^{-1}. Conformational energy calculations predicted that the crystalline material would assume an all-trans conformation while the liquid would comprise of a mixture of tttt and ttg^+g^+ states. For the racemic dimer, two peaks were observed at 751 and 791 cm^{-1} and were assigned to tt and g^+g^+ conformations, respectively. Conversely iPS, the meso dimer, and the isotactic trimer gave rise to only one peak at 798, 787, and 780 cm^{-1}, respectively.

Our work confirms such assignments of the peaks observed at 769−773 and 796−802 cm^{-1}, respectively. Analysis of a polished cross section of a compression-molded plaque, which was quenched in ice water to induce a glassy skin/crystalline core structure, showed a clear continuous relationship between these two peaks. A clearer view of the observed changes is shown in Figure 7 where the ratio of the intensities of the ν_1 peaks (I_{773}/I_{798}) is plotted against distance from the skin. As crystallinity increases (from skin to core), the weaker peak at 770 cm^{-1} grows in intensity at the expense of the initially strong peak at 798 cm^{-1} resulting in an increase in the ratio value from ∼0.3 (skin) to ∼3.8 (crystalline core). For comparison, the ratios of intensities for the reference glassy sample and the fully annealed, highly crystalline sample are 0.3 and 3.8, respectively. It would appear from Figure 7 that the crystallinity reaches a maximum at ∼500 μm and then decreases slightly. This can be explained in terms of processing conditions/thermal history during production of the plaque. Analysis of the reference glassy and crystalline sPS samples shows that the position of the low-frequency peak shifts up in frequency from 770 to 773 cm^{-1}, while the 797 cm^{-1}, peak moves down slightly to 796 cm^{-1} and analogous behavior is observed for the molded material, Figure 8. The full width at half-height of the low-frequency peak decreases with increasing crystallization (∼14−∼7 cm^{-1}) as would be expected for such a packing sensitive conformation. The variation of the width of the 798−796 cm^{-1} peak (∼14 cm^{-1}) is not considered significant within the experimental error. Analysis of the spectra obtained from the molded plaque closely mirrors these changes described above, Figure 9.

Some differences are observed, especially in the width of the all-trans ν_1 peak between the reference glassy material and the skin of the molded plaque. For the reference material, the peak is observed to be much broader. This can be explained in terms of the thermal history for the two samples: The reference material is much thinner (300 μm) and therefore would cool quickly during production, whereas the plaque is much thicker resulting in delayed quenching and therefore slightly higher crystallinity as heat diffuses from the core.

Atactic PS was also analyzed (Figure 5), and a similar spectrum to that of glassy sPS (Figure 2) was derived. Curve fitting implied the possibility of the presence of two ν_1 vibration peaks at 796 and 769 cm^{-1}. The former strong peak is assigned to trans/gauche conformations with an increased peak width over sPS (∼19 cm^{-1}) reflecting the much more random nature of aPS. The presence of a peak, albeit weak and very broad (∼20 cm^{-1}), at 768 cm^{-1} is evidence of a small population of syndiotactic all-trans sequences within the polymer. The presence of 'syndiotacticity' in aPS is well known, and NMR[21] and infrared spectroscopy[22] have been used in the past to study such sequences. To our knowledge this is the first time that the ν_1 peaks in the Raman spectrum have been correctly assigned to aPS. Jasse et al.[19] have assigned two peaks to the ν_1 mode for aPS, one at 797 cm^{-1} and the other at 763 cm^{-1}, and they were assigned to $(tttt)_n$ sequences and shorter all-trans sequences, respectively. However, in the light of our data and curve analysis, we feel that our assignments are more consistent. All other spectral features in this region are shown to be very stable in position and hence less liable to misassignment. Similar peaks (772 and 793 cm^{-1}) have also been reported by Sears et al.[23] in the case of partially polymerized styrene; however, only the 793 cm^{-1} feature was assigned to the ν_1 vibration with the 772 cm^{-1} peak being attributed to ν_1 for styrene monomer. In the case of the samples studied here, the presence of styrene monomer is not observed.

Table 2 shows our revised assignments for the peaks derived from the ν_1 vibration, and an upward frequency shift can be observed as the length of the all-trans conformation of a syndiotactic sequence increases from

Table 1. Vibrational Assignments for Polystyrene and Model Compounds within 600−800 cm^{-1} Region of Raman Spectrum[a]

Herzberg	ν_{18}	?		ν_8		ν_4	ν_2	ν_2		ν_{11a}
Wilson	ν_{6b}	?	$CHCl_3$	ν_4	$\nu_{10b} + \nu_{16b}$	ν_{11}	ν_1 (tt...)	ν_1 (t/g..)	$\beta_{as}(CH_2)$	ν_{10a}
dimer (meso)[b]	623				740	760		780 (tg^+)		844
dimer (racemic)[b]	623				740	765 sh	751	791 (g^-g^-)		843
trimer (isotactic)[b]	623				740	763		787 (tg^+tg^+)		843
trimer (heterotactic)[b]	623				740	763	750	781 (tg^+(tt), g^-t(tt), $g^-tg^-g^-$)		843
trimer (syndiotactic), liquid[b]	623				740	763	763	789 ((tt^+)g^+g^+)		843
trimer (syndiatactic), crystal[b]	623				740	763	763			845
iPS[b]	623				740	768		789 ((tg^+)$_n$)		844
aPS[b]	623				740	762	763 (ttt?) 797 ((tt)$_n$)			846
sPS, trans (crystal)[c]	622			703	740	756	773	796	811	841
sPS (glass)[c]	622	636		699	741	757	770	798	811	841
sPS, helical (crystal)[c]	622	636	670	702	745	758	772	802	812	840
aPS[c]	622			703	741	756	769	796	813	841

[a] Note: dimer refers to 2,4-diphenylpentane and trimer refers to 2,4,6-triphenylheptane. [b] Data from Jasse et al.[19] [c] Our data.

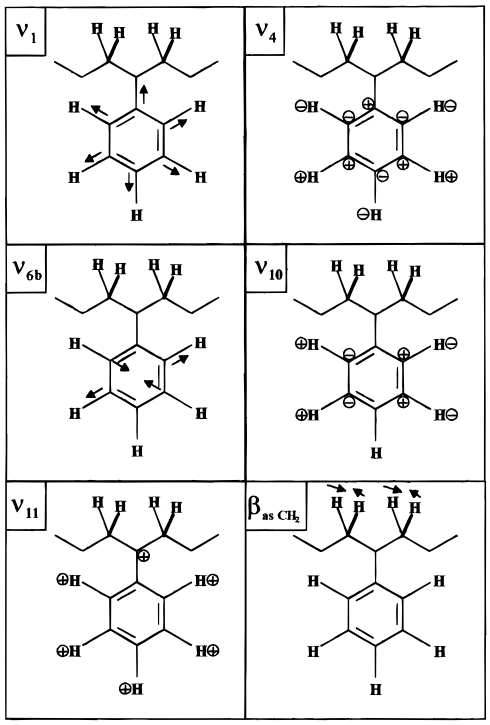

Figure 6. Normal vibrational modes of polystyrene present between 600 and 850 cm^{-1}. Symbols ⊖ and ⊕ denote motion into and out of the plane of the paper, respectively.

751 cm^{-1} (tt) to 773 cm^{-1} $(tttt)_n$. The higher frequency trans/gauche peak is much less sensitive to position due to its more random nature. Also included in the table are the observed peak widths at half-height for sPS and aPs which show a narrowing with increasing lengths of all-trans sequences.

Peak analysis of the helical crystal forms of sPS, Figure 4, shows that there is virtually no difference between the γ and δ polymorphs within this spectral window with the exception of the presence of a chloroform peak for the δ polymorph. However comparison with the glassy and melt-crystallized material shows the effect that alteration of a regular backbone conformation can have on the ν_1 vibrational features. The main peak at 802 cm^{-1} is clearly associated with the mixture of trans and gauche conformations; however, the shift to higher frequencies and the narrowness of the band (10.5 cm^{-1}) as compared with the other spectra (Figures 2, 3, and 7) would imply that a regular crystalline sequence of ttg^+g^+ sequences is present. At ∼772 cm^{-1}, a weaker broad peak, 15.4 cm^{-1}, can be identified and

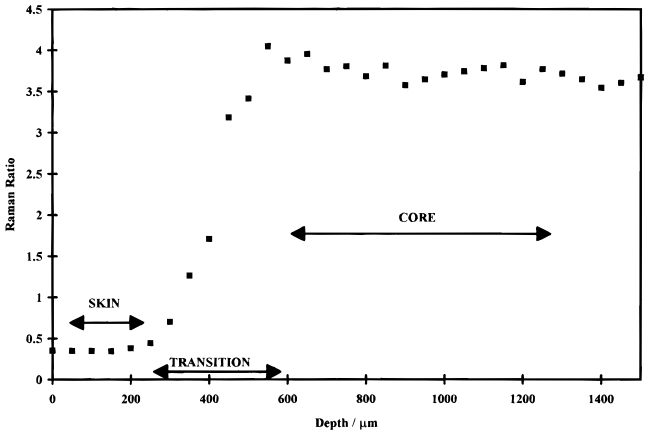

Figure 7. Variation of Raman intensity ratio of ν_1 peaks (I_{773}/I_{798}) at points along a section of a molded plaque from skin to core.

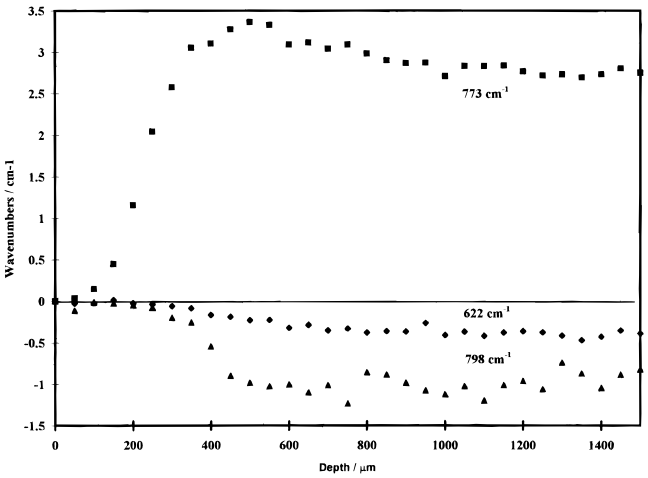

Figure 8. Relative positional shifts of the Raman features at 622, 773, and 798 cm^{-1} from skin to core of a molded plaque.

is assigned to long isolated trans sequences within the material. The frequency of the peak (∼773 cm^{-1}) denotes long sequences, but the broad bandwidth implies low crystallinity.

Assignment of the Other Vibrational Features. Curve fitting analysis of all the spectra (Figures 2−5) together with an extensive literature[6,17,23−27] survey results in the assignments made in Table 1. All of these peaks were shown to be positionally stable for all the samples analyzed thus reducing ambiguity. The only peaks not due to normal vibrational modes are observed

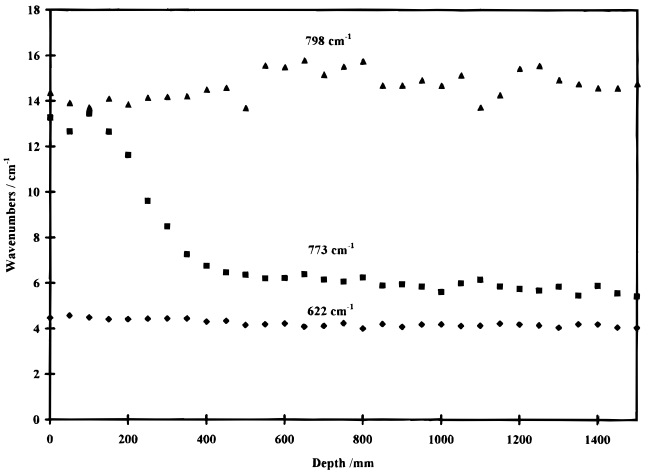

Figure 9. Variation in band width at half-height for 622, 773, and 798 cm^{-1} peaks at points along a section of a molded plaque from skin to core.

at 740 and 636 cm^{-1}. The first of these has been assigned by Jasse et al.[19] to a combination of two B_1 modes, ν_{10b} and ν_{16b}. (190 cm^{-1} + 550 cm^{-1} = 740 cm^{-1}). However it has not been possible at this stage to assign the weak feature at 636 cm^{-1} seen in the spectra of glassy and helical sPS (Figures 2 and 4). The peak at 622 cm^{-1}, due to the ν_{6b} vibration, is very substituent insensitive and is observed at virtually the same position (within 2 cm^{-1}) for all polystyrenes and related analogues thus making it ideal as a positional calibration peak. Such stability is clearly demonstrated throughout the whole of the injection-molded sample as shown in Figure 8. The 622 cm^{-1} peak has also been found to have almost constant intensity and peak width (Figure 9) for aPS and sPS thus allowing a scaling factor to be applied to all spectra studied. For the helical sPS sample (Figure 4), a peak can be observed at 670 cm^{-1} which is due to the presence of chloroform still locked within the crystal structure.

Optical Studies. In order to verify the change in crystallinity through the injection-molded plaque, a thin section was examined between crossed polarizers under the microscope, and a close correlation can be seen between the Raman ratio data (Figure 7) and a photograph of a similar region, Figure 10a. A dark (nonbirefringent) skin is seen to extend for ~300 μm followed by a region of increasing birefringence (~250 μm) to a highly birefringent crystalline core. The dimensions are not exactly consistent with the Raman ratio data, Figure 7, due to variations of skin thickness along the plaque's length and to the presence of very small nonbirefringent crystallites which are below the resolution of the optics employed in this study, thus making the glassy skin appear thicker than what would be expected from Raman studies. However the transition between glassy skin and crystalline core can easily be followed. Close examination at higher magnification, Figure 10b, reveals an isotropic spherulitic morphology with spherulites growing in size with diameters ranging from ~1 to ~8 μm. In the transition region, individual isolated spherulites can be observed surrounded by nonbirefringent, glassy material. It is this mixture of crystalline and glassy morphologies which accounts for the slight discontinuities of the Raman ratio values observed in this region as the small laser spot size (~2 μm) may traverse both spherulitic and glassy material, Figure 7. As the core is approached, the spherulites impinge on each other and their dimensions are less easily defined.

Raman Spectroscopy versus Infrared Spectroscopy. The preliminary work described in this paper involving the analysis of changes in crystallinity of a molded sample clearly demonstrates a number of advantages that the Raman microscope has over the equivalent infrared equipment in the study of sPS. As the polymer is relatively stable, high laser power can be used (~ 15mW) without damaging the material thus enabling rapid collection of spectra (~45 s). To obtain a spectrum of equivalent resolution and signal to noise ratio using the FTIR microscope, the time scale would be in the order of several minutes at best. The current minimum spot size diameter for the FTIR microscope is of the order of 10 μm, whereas ~1 μm is routine for the Raman microscope; this therefore allows for greater resolution when mapping spectra across the sample surface. The use of a pinhole, positioned on the back focal plane of the microscope enables the Raman microscope to be adapted for confocal studies. This enables spectra to be obtained below the surface of the sample and is limited only by the scattering character of the material under analysis. Finally comparison of the two types of spectra reveals that the Raman spectrum is much less complex with well-defined sharp features, thus enabling accurate base-line definition and easier, more accurate spectral analysis to be performed.

Conclusions

A complete analysis has been made of the normal vibrational modes making up the Raman spectrum of sPS and aPS in the region 600−850 cm^{-1}. The spectral profile of the two polymers is very similar differing only with respect to the position and relative intensity of the peaks corresponding to the ν_1 vibration. It has been clearly demonstrated that the highly symmetric nature of the ν_1 vibration is sensitive to the conformation of the backbone and that of its immediate neighbors. In the case of polystyrene, this is evidenced by the presence of two strong and highly polarized peaks. Previously published work on model compounds has shown that the lower frequency vibration is due to all-trans sequences (α/β crystal polymorphs) while the higher frequency peak results from a mixture of trans and gauche states. The latter can therefore be attributed to the amorphous component of sPS provided its position

Table 2. Revised ν_1 Assignments, Peak Positions, and Peak Widths for Syndiotactic *n*-Styrene Compounds

				sPS		
					crystal	
dimer (racemic)		trimer (syndiotactic)	aPS	glass	planar zigzag	helical
751	position, cm^{-1}	763	769	770	773	772
tt	conformation	tttt	(tttt...)	$(tttt)_n$	$(tttt)_m$, where $m > n$	$(tttt)_m$, where $m > n$
n/a	width, cm^{-1}	n/a	~20	~14	~6	~16
791	position, cm^{-1}	789	796	798	796	802
tg	conformation	(t,g)	(t,g)	(t,g)	(t,g)	(ttg^+g^+)
n/a	width, cm^{-1}	n/a	~19	~14	~14	~11

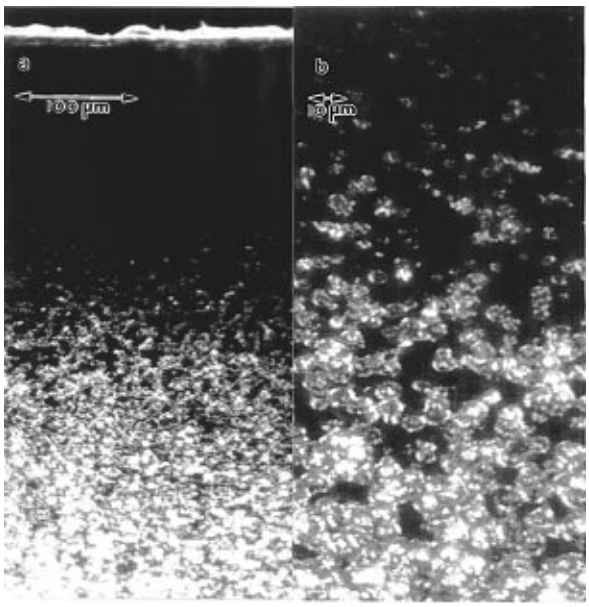

Figure 10. (a) Ultramicrotomed section of compression-molded sample viewed between crossed polarizers showing a nonbirefringent skin (dark) changing to a fully crystalline core (bright) via an intermediate transition region. (b) Magnified intermediate transition region.

is not shifted to values >800 cm^{-1}, which is observed only when long ttg^+g^+ sequences are present resulting in a crystalline helical structure (γ/δ crystal polymorphs). The lower frequency peak at 770−773 cm^{-1} is observed to grow and narrow into an intense feature upon crystallization. The presence of two ν_1 peaks for aPS reaffirms previous studies using other methods that there is a significant syndiotactic component present within the atactic polymer.

The continuity of these observed changes was demonstrated through analysis of a glassy skin/crystalline core sample. It has been shown that Raman spectroscopy can provide valuable information about the level of crystallinity together with the type of backbone conformation present within sPS samples. Study of a polished cross section by taking spectra at set intervals from skin to core underlines the power of this technique. In order to make the observed changes quantifiable in terms of crystallinity, it is essential to study material of intermediate crystallinity which can be analyzed using more direct techniques such as XRD and/or DSC. This will be the subject of the second paper of the series.[28]

Acknowledgment. The authors would like to express their thanks to Mike Cook and Thomas Wegman (Dow Chemicals, Terneuzen, Holland), Craig Carriere (Dow Chemicals, Midland,TX), Bob Dyson (University of North London Polymer Technology Unit), and Angus Evans (The Raman Group, QMW) for their help with supplying materials and sample preparation.

References and Notes

(1) Ishihara, N.; Seimiya, T.; Kuramoto, M.; Voi, M. *Macromolecules* **1986**, *19*, 2464.
(2) Guerra, G.; Vitagliano, V. M.; De Rosa, C.; Petraccone, V.; Corrandini, P. *Macromolecules* **1990**, *23*, 1539.
(3) Corradini, P.; Guerra, G. *Adv. Polym. Sci.* **1992**, *100*, 183.
(4) Doherty, D. C.; Hopfinger, A. J. *Macromolecules* **1989**, *22*, 2472.
(5) Greis, O.; Xu, Y.; Asano, T.; Petermann, J. *Polymer* **1989**, *30*, 590.
(6) Sun, Z.; Millar, R. L. *Polymer* **1993**, *34*, 1963.
(7) De Rosa, C.; Guerra, G.; Petraccone, V.; Corradini, P. *Polym. J.* **1991**, *23*, 1435.
(8) De Rosa, C.; Rapacciuolo, M.; Guerra, G.; Petraccone, V.; Corradini, P. *Polymer* **1992**, *33*, 1423.
(9) Chatani, Y.; Shimane, Y.; Inagaki, T.; Ijitsu, T.; Yukinari, T.; Shikuma, H. *Polymer* **1993**, *34*, 1620.
(10) Reynolds, N. M.; Savage, J. D.; Hsu, S. L. *Macromolecules* **1989**, *22*, 2867.
(11) Filho, A. R.; Vittoria, V. *Makromol. Chem., Rapid Commun.* **1990**, *11*, 199.
(12) Guerra, G.; Musto, P.; Karasz, F. E.; MacNight, W. J. *Makromol. Chem.* **1990**, *191*, 2111.
(13) Nakaoki, T.; Kobayashi, M. *J. Mol. Struct.* **1991**, *242*, 315.
(14) Kobayashi, M.; Nakaoki, T.; Ishihara, N. *Macromolecules* **1990**, *23*, 78.
(15) Reynolds, N. M.; Stidham, H. D.; Hsu, S. L. *Macromolecules* **1991**, *24*, 3662.
(16) Reynolds, N. M.; Hsu, S. L. *Macromolecules* **1990**, *23*, 3463.
(17) Nyquist, R. A.; Putzig, C. L.; Leugers, M. A.; McLachlan, R. D.; Thill, B. *Appl. Spectrosc.* **1992**, *46*, 981.
(18) Kobayashi, M.; Nakaoki, T.; Ishihara, N. *Macromolecules* **1989**, *22*, 4377.
(19) Jasse, B.; Chao, R. S.; Koenig, J. L. *J. Raman Spectrosc.* **1979**, *8*, 244.
(20) Kellar, E. J. C.; Galiotis, C.; Andrews, E. H. Unpublished data.
(21) Jasse, B.; Laupretre, F.; Monnerie, L. *Makromol. Chem.* **1977**, *178*, 1987.
(22) Jasse, B.; Koenig, J. L. *J. Polym. Sci. Polym. Phys. Ed.* **1978**, *16*, 1869.
(23) Sears, W. M.; Hunt, J. L.; Stevens, J. R. *J. Chem. Phys.* **1981**, *75*, 1589.
(24) Varsanyi, G. *Vibrational Spectra of Benzene Derivatives*; Academic Press: New York, London, 1955.
(25) Liang, C. Y.; Krimm, S. *J. Polym. Sci.* **1958**, *27*, 241.
(26) Onishi, T.; Krimm, S. *J. Appl. Phys.* **1961**, *32*, 2320.
(27) Painter, P. C.; Koenig, J. L. *J. Polym. Sci., Polym. Phys. Ed.* **1977**, *15*, 1885.
(28) Kellar, E. J. C.; Evans, A.; Galiotis, C.; Andrews, E. H. Manuscript in preparation.

MA950772T